AIMS Materials Science, 11(2): 323–342.
DOI: 10.3934/matersci.2024018
Received: 17 January 2024
Revised: 29 February 2024
Accepted: 11 March 2024
Published: 20 March 2024

http://www.aimspress.com/journal/Materials

Research article

The effect of polyaniline composition on the polyurethane/polyaniline composite properties: The enhancement of electrical and mechanical properties for medical tissue engineering

Dhonluck Manop[1,*], Chaileok Tanghengjaroen[1], Chatchai Putson[2] and Panya Khaenamkaew[1]

[1] Department of Basic Science and Physical Education, Faculty of Science at Sriracha, Kasetsart University, Sriracha Campus, Chonburi, Thailand, 20230
[2] Division of Physical Science, Faculty of Science, Prince of Songkla University, Songkhla, Thailand, 90110

* **Correspondence:** Email: dhonluck.m@ku.th; Tel: +66-890-106-898.

Abstract: This study addresses the urgent need for the preparation and characterization of conductive polyurethane/polyaniline (PU/PANI) polymers for medical device applications, particularly in the context of the COVID-19 situation. Composite films of PU/PANI were synthesized using the solution casting method. Fourier-transform infrared (FT-IR) results confirmed the presence of PANI, as indicated by absorption bands at 1597 and 1531 cm^{-1} corresponding to C=C and C–N stretching, respectively. Microscopic analyses using scanning electron microscopy (SEM) and atomic force microscopy (AFM) demonstrated a homogeneous distribution of PANI in the PU matrix up to approximately 3 wt.%, with inhomogeneity observed at 5 wt.%. The dielectric constants at 1 Hz for PANI contents of 1, 3, and 5 wt.% in the PU matrix were 12.5, 18.5, and 35.0, respectively. The conductivity exhibited a decreasing trend with an increasing driving frequency. Conversely, for comparative purposes, the dielectric and conductivity values increased with higher PANI contents. The elastic modulus slightly increased from 20.3, 20.8, and 21.2 for 1, 3, and 5 wt.%, respectively. The experimental results emphasize the superior mechanical-to-electrical conversion performance of PU/PANI composites compared to neat PU, thus indicating potential applications in medical tissue engineering that utilize conductive PU/PANI polymers.

Keywords: polyurethane/polyaniline composite; electrical properties; mechanical properties; elastic modulus; medical tissue engineering

1. Introduction

With the ongoing emergence of new evidence regarding SARS-CoV-2, there is a heightened interest and demand for medical technologies and their supply chain. As part of technological advancements, traditional medical materials such as metals and alloys are being substituted with polymers. As reported by Grand View Research, the global bio-based polyurethane (PU) market recorded 1.534×10^6 kg in 2012 and nearly USD 19.5 billion in 2015, exhibiting an annual growth rate of 8.5%. Moreover, the global polyurethane foam market size, estimated at USD 43.70 billion in 2023, is projected to grow at a compound annual growth rate (CAGR) of 7.8% from 2024 to 2030 [1]. PUs inherently possess a blend of durability and toughness reminiscent of metals, along with the elasticity of rubber. This unique combination positions them as suitable substitutes for metals, plastics, and rubber in various engineered products.

Electroactive polymers (EAPs) are considered intelligent materials that can respond to external voltage stimuli and demonstrate substantial deformations [2,3]. Renowned as prominent electroactive polymers, polyurethane/polyaniline composites (PU/PANI) find extensive applications in the medical field owing to their remarkable biocompatibility, electrical conductivity, mechanical properties, drug delivery capabilities, and antimicrobial properties [4]. They are well-tolerated by the body, conduct electricity for signal transmission, withstand stress and deformation, enable controlled drug release, prevent infections, and find applications in catheters, wound dressings, and surgical implants [5]. In the current scenario, although PU/PANI composites show promise for medical applications, several research gaps remain. According to the literature, PU/PANI medical applications require excellent electrical and mechanical characteristics.

Known for its flexibility, biocompatibility, and resilience, PU has been extensively employed in medical devices and implants [3]. However, the inherent limitations of PU, such as modest electrical conductivity, necessitate innovative strategies for enhancement. In tandem, PANI, a conducting polymer renowned for its high electrical conductivity and environmental stability, presents itself as a compelling candidate for synergistic integration with PU [4]. As a versatile polymer, PANI can be synthesized in various forms with distinct properties determined by its oxidation level. These forms include pernigraniline (black and oxidized), emeraldine in insulating (emeraldine base (EB)) (blue) or conductive salts (emeraldine salt (ES)) [6] (green and half-oxidized), and leucoemeraldine (pale and reduced) [7]. PANI's structure is comprised of repeating units of the monomer aniline, thus forming a long backbone with alternating single and double bonds. The N-atom between the phenyl rings allows the polymer to exist in different oxidation states, influencing its physicochemical and mechanical properties significantly [8]. The intersection of PU and PANI opens avenues to tailor materials with augmented electrical and mechanical attributes, which are crucial for addressing the multifaceted requirements of medical applications. The enhancement of electrical conductivity is imperative for applications such as sensors and actuators [2–4,9], while optimizing mechanical properties is essential for ensuring compatibility with biological tissues, durability, and overall performance in medical contexts [8,10,11].

Despite advancements in the field, a comprehensive understanding of the intricate interplay between PANI and PU, specifically in the context of medical applications, remains elusive. Existing literature hints at the potential of such composites but falls short of providing a nuanced exploration of the material characteristics necessary for optimal performance in medical settings.

Numerous studies have explored the fabrication and properties of PU and PANI composites. PU/PANI composites were successfully processed and characterized for stress sensing applications using ultra-high molecular weight polyethylene (PE-UHMW). The confirmation of effective particle distribution in the composites was achieved through various analytical techniques, including Fourier-transform infrared (FT-IR) spectroscopy, thermogravimetric analysis (TGA), differential thermal analysis (DTA), scanning electron microscopy (SEM), and energy-dispersive X-ray spectroscopy (EDS). Piezoresistive characterization revealed that the operating voltage had a significant impact on the hysteresis and drift error metrics. While higher voltages resulted in reduced errors, they also contributed to a decrease in sensor sensitivity. A microscopic model was developed to elucidate the piezoresistive response of PANI composites, thereby aiming to enhance their applicability in strain/stress sensing applications as an alternative to carbonaceous materials [9].

Putson et al. [12] conducted an investigation into the impact of the copper (Cu) filler size and content on both the dielectric and mechanical properties of polyurethane, utilizing a solution casting technique. Their study revealed distinct dispersion behaviors, wherein microparticles demonstrated a relatively uniform dispersion, while nanoparticles tended to aggregate, thus resulting in poor compatibility. Additionally, a dielectric analysis indicated a direct correlation between the filler content and the dielectric constant, with a higher filler content leading to an increase in dielectric constant. Regarding the mechanical properties, an overall increase in the tensile modulus was observed with a rising Cu content, which was particularly evident with microparticles. Conversely, composites containing nanoparticles exhibited a gradual decrease in the tensile strength as the filler content increased, contrasting with the more substantial decline observed with microparticles. These findings underscore the significant influence of filler size and content on the dielectric and mechanical characteristics of polyurethane composites. In a similar vein, Pierini and his colleague explored hybrid organic-inorganic fibers that incorporated geomimetic chrysotile nanotubes and multiwalled carbon nanotubes (MWCNTs), thus resulting in a notable enhancement in the electrical conductivity. Notably, chrysotile-filled fibers exhibited a superior conductivity attributed to the oriented arrangement of nanotubes and a heightened crystallinity. These advancements hold promise for various applications in molecular electronics and the development of strategic materials [13].

Furthermore, Pierini and his co-worker elucidated the electrical properties of polyaniline emeraldine base/silver nitrate/1-butanethiol (PANIAg-BuT) nanocomposites compared to PANIAg-4-methylbenzenethiol (MBT), thus emphasizing the crucial role of the thiol layer structure in determining the electrical conductivity. These insights underscore the significance of the tailored metal nanoparticle core composition and thiol protecting layer structure to achieve the desired electrical properties in conjugated polymer-based nanocomposites [13,14]. However, despite the potential of metals such as copper to enhance conductivity, their usage in medicinal materials remains limited. To overcome this constraint, PANI emerges as a crucial electrical additive material. The ongoing advancements in the electrical and mechanical properties of PU have facilitated innovative developments, such as the fabrication of fibers that utilize PU/PANI composites with varying PANI loadings.

The aforementioned literature provides the primary conclusion that PU maintains the desired mechanical properties. Additionally, it emphasizes that the dielectric constant and electrical conductivity

of PU/PANI are significantly influenced by their composition, as observed in the study conducted by Putson, Jaaoh, and Muensit in 2013 [15]. However, ambiguity persists, particularly concerning the maximum limit of PANI that can be incorporated into the PU host while still maintaining high electrical properties and preserving the favorable elastic modulus. In particular, the addition of up to 1 wt.% PANI to the PU matrix led to significant improvements in the thermal properties. PANI increased the glass transition temperature (T_g), melting temperature (T_m), and degradation temperature, thus enhancing thermal stability. PANI loading in PU blends an increased thermal stability up to 339 °C [16]. Additionally, the mechanical properties, such as tensile strength and elastic modulus, were improved with the addition of PANI [17]. Simultaneously, the mechanical properties of the PU matrix, including the tensile strength and elastic modulus, saw positive effects with PANI incorporation. Additionally, the electrical conductivity of PU/PANI blends showed a direct correlation with PANI loading, thus indicating an increasing conductivity with higher PANI content. Apart from thermal and mechanical enhancements, the blends exhibited remarkable recoverability in thermally triggered shape memory behavior. Notably, the 1 wt.% PANI blend achieved an impressive 96% recovery extent, thus emphasizing the potential for tailored shape memory characteristics in these composites [18]. These findings suggest that the composition of PANI in PU blends can be optimized to enhance the electrical and mechanical properties of the material for medical applications. To the best of our knowledge, no report about a combination of PANI into PU above 3 wt.% has been published in the literature.

As we previously mentioned certain research gaps, optimizing the mechanical and electrical properties of PU/PANI composites is pivotal for their successful application in tissue engineering. The expected dielectric constant of PU/PANI composites is higher than reported in the literature, all the while maintaining their excellent elastic modulus [19]. The versatility of these properties opens up possibilities for innovative solutions in the medical field, contributing to improved patient care and treatment modalities.

The primary objective of this study is to clarify the intricate process of integrating PANI into PU, thus leading to advanced PU/PANI composite materials. By employing a comprehensive approach, including morphological and molecular vibration analyses, this investigation aims to delve into the structural nuances of the resulting composites. Additionally, this study seeks to systematically enhance the electrical and mechanical properties of PU by exploring the effect of varying 1, 3, and 5 wt.% of PANI. This research aims to bridge the existing gaps in understanding the optimal integration of these materials for medical applications. The outcomes are expected to contribute not only to fundamental knowledge, but also pave the way for practical applications. Specifically, this research aims to provide valuable insights into the viability of these materials for applications in energy harvesting, thereby advancing their utility in the medical field.

2. Materials and methods

2.1. Samples preparation

PU/PANI composites were prepared by the solution casting method based on the International Union of Pure and Apply Chemistry technical report (IUPACT) [20]. PU granules (Estane 58888-NAT 021, Lubrizol Corp.) and PANI powder (Emeraldine Salt, Sigma-Aldrich 561134) were used as starting materials. PU granules were dissolved in N, N-Dimethylformamide (DMF, 99% purity, D158550

Sigma Aldrich) solvents at 80 °C for 45 min as a matrix. PANI powders were ultrasonically dispersed in the DMF solution for 20 min and used as the filler of the PU matrix.

The PANI solution was added to the PU matrix solution under a mechanical stirring condition and heated at 80 °C for 45 min to obtain a homogeneous PU/PANI solution. This viscous mixture (PU/PANI solution) was cast onto the glass substrate and cured at 80 °C for 24 h. The films were removed from the glass and annealed at 80 °C for 3 h. Finally, the thickness of the obtained films was approximately 80 μm. To investigate the influence of the PANI composition on the PU characteristics, the weight fraction of the fillers inside the composites was changed from 0 (so called neat PU) to 1, 3, and 5 wt.%. The weight fraction was calculated using the components solid densities.

2.2. Characterizations

The FT-IR spectrometer (Bruker, Model INVENIO R with OPUS software) was used to examine the molecular structure of the complicated PU/PANI mixtures. All samples were measured using the attenuated total reflectance accessory (Single Deflection Diamond ATR accessories). SEM is widely used to investigate the morphology and topography of conductive and non-conductive materials. A scanning electron microscope was used to investigate the microstructure of the PU/PANI composites (SEM, VEGA3 TESCAN MIRA3 XMU). Gold sputtering was applied to the entire samples prior to SEM imaging, with an accelerating voltage of 20 kV. The particle size distribution analysis of the SEM images was conducted using the ImageJ software (version 1.8.0), which is an open-source image analysis tool widely utilized in scientific research. At room temperature, the topographical samples were examined using atomic force microscopy (AFM, Nanosurf, Nanosurf Easy Scan 2, Switzerland) in a tapping mode.

The dielectric property yields crucial insights into the storage and dissipation of electric fields in conductive polymers, thus determining their suitability for various applications. The dielectric constant, also known as the relative permittivity (ε_r) or absolute permittivity (ε), is expressed in relation to the permittivity of free space (Eqs 1–3). It is a complex quantity that characterizes the interaction between a substance and an electric field [21].

$$\varepsilon = \varepsilon' - j\varepsilon'' = \varepsilon'(1 - j\,tan\,\delta) = \left|\varepsilon'\right|e^{-j\delta} \tag{1}$$

$$\varepsilon' = \varepsilon_0\varepsilon_r \tag{2}$$

$$\varepsilon'' = \varepsilon' tan\,\delta \tag{3}$$

The real portion of permittivity (ε') is a measure of how much energy is stored in a material as a result of an external electric field. In comparison, the imaginary portion of permittivity (ε'') is known as the loss factor and is used to determine how dissipative or lossy a material is in the presence of an external electric field. The loss factor takes the dielectric loss and the conductivity into account.

The parallel plate technique was used to test the dielectric properties of the required PU/PANI samples as a function of the PANI concentration [22]. To create a capacitor, a thin sheet of material was sandwiched between two electrodes using the parallel plate technique. The measurement's equivalent circuit was reported elsewhere. In this study, two electrodes were designed with a sandwiching test fixture and measured using an LCR analyzer (IM 3533 HIOKI, Japan) in the

frequency range of 10^0–10^5 Hz. The LCR analyzer can measure the parallel capacitance (C_p) and the dissipation (D) vector components and calculate the permittivity and loss tangents as follows:

$$\varepsilon' = \frac{tC_P}{A\varepsilon_0} \tag{4}$$

$$\varepsilon'' = \frac{t}{\omega R_P A\varepsilon_0} \tag{5}$$

In the given Eqs 4 and 5, 't' represents the thickness of the material, 'R_p' denotes the parallel resistance, 'ω' signifies the angular frequency of the driving signal, and 'A' represents the area of the PU/PANI samples.

The elastic modulus of each composite was evaluated in a strain gauge setup, with the help of a force gauge (BFG50N, Mecmesin, UK). The sample strips were cut into 30 mm long, 5 mm wide, and approximately 80 mm thick strips, and were stretched in the lengthwise direction to a 5% strain maximum at a 5 mm·min^{-1} elongation rate. The fixed end of the sample was clamped to a force sensor, while the other end was clamped to a linear motor moving stage (RC ROBO-Cylinder Model RCP 2CR-SA6, 220 mm-long) that was controlled with a function generator. The elongation versus the force curves were determined for all samples and their elastics moduli (ξ) were calculated. The strain induced by an electric field in polarizable materials, denoted as S_3, generally adheres to the following correlation:

$$S_3 = M_{33}E^2 \tag{6}$$

In this context, M_{33} represents the apparent electrostrictive coefficient governing the strain in the thickness direction under the influence of the applied electric field. Empirically, the intrinsic electrostrictive coefficient, as defined in Eq 6, demonstrates an inverse proportionality to the product of the elastic modulus and the dielectric permittivity. Hence, in the case of a dielectric material where $\varepsilon_r >> 1$, M_{33} is directly proportional to the dielectric constant and inversely proportional to the elastic modulus of the material. Eq 7 distinctly indicates the necessity for a well-calibrated balance between the dielectric constant and the material's softness to achieve an optimal electromechanical activity [23].

$$M_{33} = \frac{\varepsilon_0(\varepsilon_r - 1)^2}{\varepsilon_r \xi} \tag{7}$$

3. Results and discussion

3.1. The existence of PANI in the PU texture

Figure 1 presents a photograph of the 3 × 3 cm^2 specimens for the neat PU, PU/1%PANI, PU/3%PANI, and PU/5%PANI composites. As the PANI concentration increases, the sample color gradually becomes darker. Figure 2 shows the FT-IR spectra of the neat PU, PU/1%PANI, PU/3%PANI, and PU/5%PANI composites. The absorption peaks of around 3320–3330 cm^{-1} were attributed to the declining urethane vibrations in the N–H group of the urethane segments. In addition, urethane linkages were given to the C=O signal at 1702 cm^{-1}. For stretching and distortion vibrations, 2851 and 1458 cm^{-1} were associated with –CH_3– and –CH_2–, respectively. The C–O–C stretching vibration of the PEG2000 segments included 1091 cm^{-1}. When PANI particles were added

to the PU host, the amine group peak was shifted to a higher frequency. Moreover, the C–N stretching vibration peaks were attributed to PU-PANI interactions [24]. Furthermore, Jiang et al. [25] hypothesized that the aromatic group and hydrogen bonds are highly polarizable, thus increasing the dielectric constant. The successful preparation of PU/PANI is evidenced by several spectroscopic features observed in the blend spectrum. Specifically, Figure 2 illustrates distinct peaks at 1510 and 1012 cm^{-1}, corresponding to symmetric and asymmetric stretching vibrations of N–C–N bonds within the urethane-aniline structure, respectively. These vibrations are indicative of the reactions occurring between the –NCO groups of PU and the NH_2 groups of PANI, as elucidated by Vaquez et al. [24]. Additionally, a notable intensity in the N–H stretching vibration at 3359 cm^{-1} suggests a significant interaction between PU and PANI components. This heightened intensity indicates enhanced crosslinking and hydrogen bonding within the blends, likely facilitated by the incorporation of PANI. Furthermore, the appearance of a distinctive absorption peak at 1668 cm^{-1}, corresponding to hydrogen-bonded carbonyl stretching vibrations, underscores the formation of hydrogen bonding and urea linkages in the PU/PANI blend. Moreover, the increased intensity of the absorption peak observed at 816 cm^{-1}, which is associated with benzene ring substitution, further supports the presence of PANI within the blend spectrum, as reported by Sattar et al. [18]. These spectroscopic findings collectively affirm the successful preparation of PU/PANI and highlight the intricate intermolecular interactions between the constituent materials.

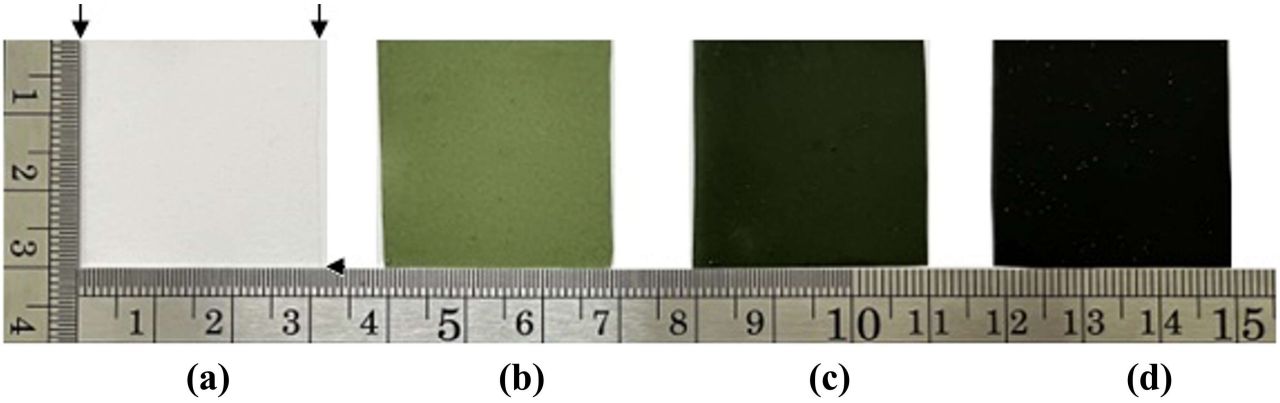

Figure 1. The photograph of PU/PANI composites samples (a) neat PU, (b) PU/1%PANI, (c) PU/3%PANI, and (d) PU/5%PANI.

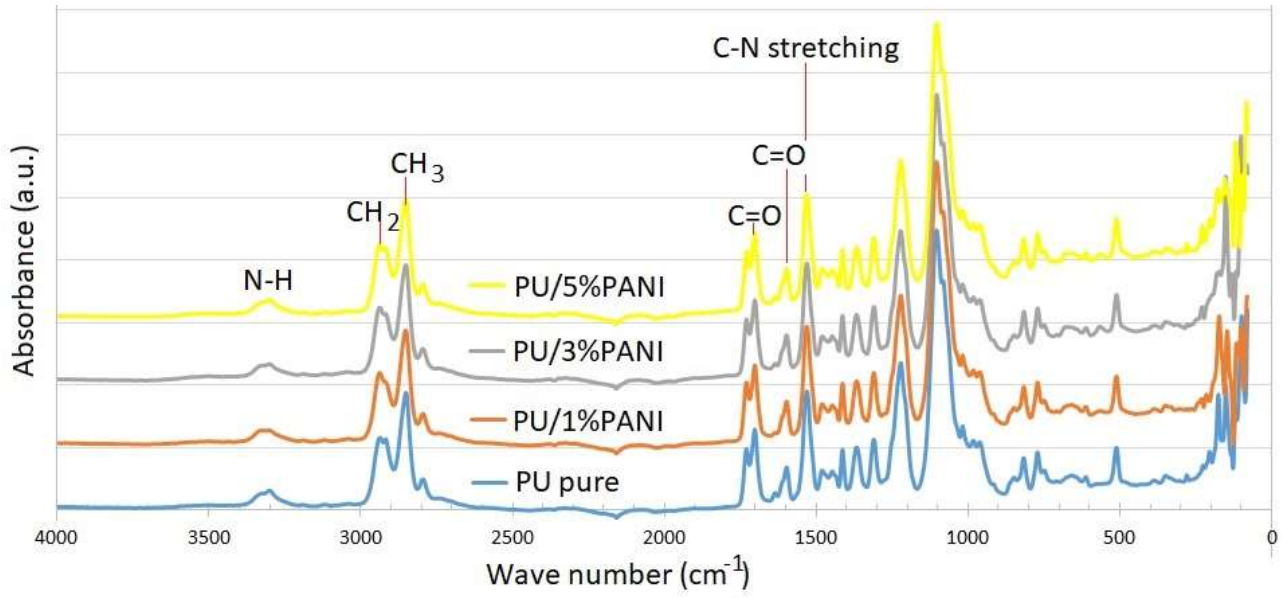

Figure 2. FT-IR spectra of PU/PANI at various PANI contents.

3.2. Effect of the PANI on the PU morphologies

Figure 3 reviews SEM micrographs of the neat PU (Figure 3a), PU/1%PANI (Figure 3b), PU/3%PANI (Figure 3c), and PU/5%PANI (Figure 3d). The PU/PANI composite appears randomly distributed for 1% and 3% PANI, with a fairly good filler dispersion. The PANI particle size was estimated to be about 0.1–5 μm in Figure 3b,c, whereas Figure 3d shows a PANI rod with a size of 20 μm long. The results in Figure 3 confirm that the agglomeration of PANI increases with an increasing PANI content. Moreover, the morphologies reveal PANI agglomeration in the mixtures with the DMF solvent, as illustrated in Figure 3a–c. However, the blend film in the DMF solvent (Figure 3d) exhibits an inadequate filler dispersion within the matrix, thus resulting in the observation of large agglomerates. This occurrence may be attributed to the filler-overloaded effect of the PU matrix and the presence of 5 wt.% PANI fillers. During the PANI preparation process, it appears that ultrasonic dispersion in the DMF solution for 20 min is insufficient for effective blending. Nevertheless, the non-homogeneous agglomeration of PU/PANI does not emerge as a primary concern for medical device applications. The presence of substantial agglomerates in the 5 wt.% PANI fillers could trigger an electric charge induction, thus generating arbitrary polarization and contributing to the heightened conductivity of PU/PANI composites. Subsequent paragraphs will detail and deliberate upon the electrical properties of the 5 wt.% PANI fillers, with a focus on their potential applications in medical devices.

The uniform dispersion of 1% PANI and 3% PANI fillers within the PU matrix is evident from the SEM images. This phenomenon is elucidated by the establishment of interfaces between PANI fillers and the PU matrix, thus leading to a substantial enhancement in interfacial polarization. The augmentation in the filler content corresponds to larger total effective interface areas, thereby contributing to the observed elevation in the dielectric constant within the low-frequency range. This finding underscores the pivotal role of interfacial interactions in shaping the electrical properties of the PU/PANI composites, thus emphasizing the significance of filler-matrix interfaces in modulating dielectric characteristics.

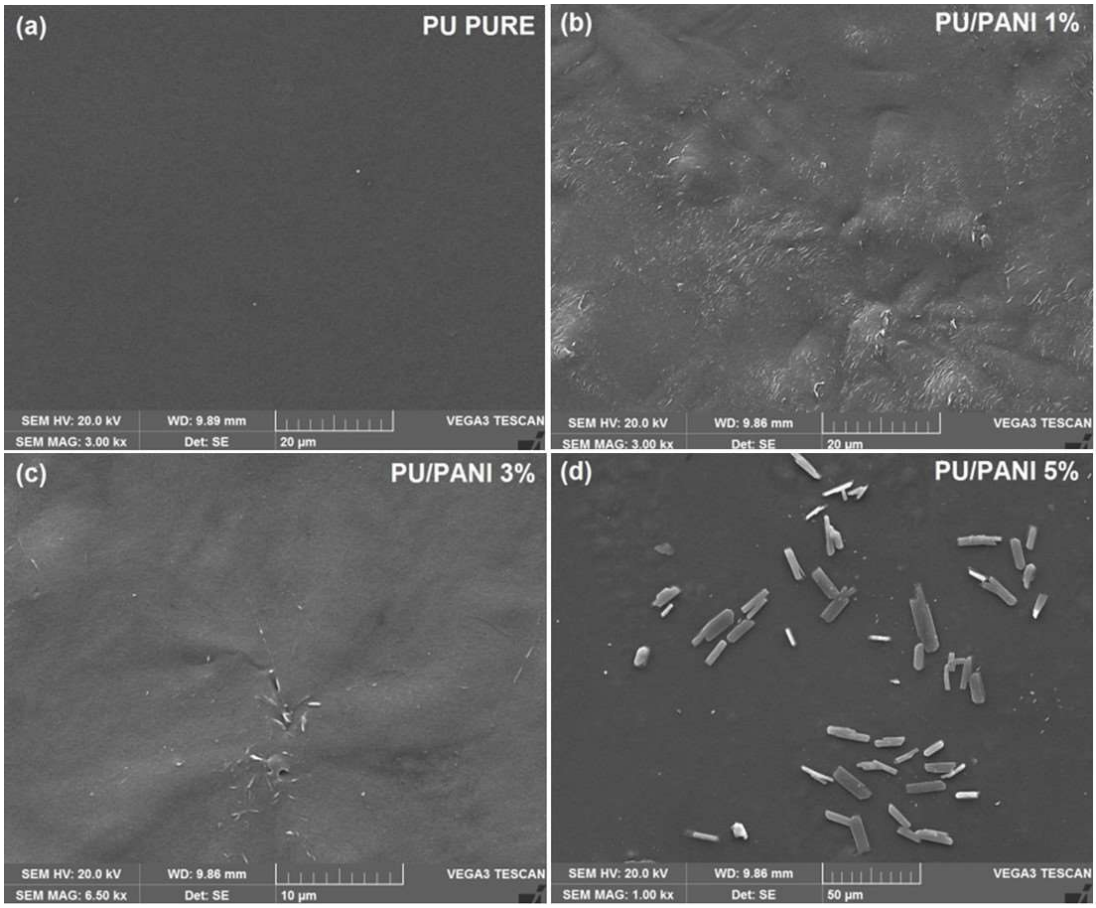

Figure 3. SEM micrographs of the PU blended with (a) neat PU, (b) PU/1%PANI, (c) PU/3%PANI, and (d) PU/5%PANI, respectively.

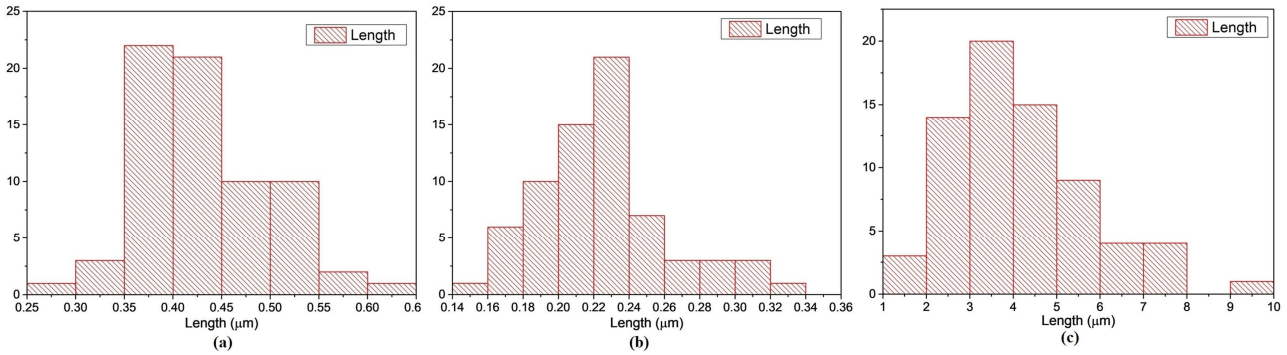

Figure 4. Particle size distribution analysis of the PU blended with PANI (a) PU/1%PANI, (b) PU/3%PANI, and (c) PU/5%PANI, respectively.

As illustrated in Figure 4a (PU/1%PANI), the particle size distribution analysis provides a detailed depiction of the particle size range present within the sample along with their corresponding frequencies. The observed microstructure reveals a variation in the particle sizes ranging from approximately 0.32 to 0.57 µm. Each size interval corresponds to a specific number of particles, thus reflecting the abundance of particles within that particular size range. For example, the data indicates

the presence of 2.5 particles with dimensions around 0.32 μm and 21 particles within the range of 0.37 μm, among others. Furthermore, Figure 4b (PU/3%PANI) showcases particle sizes ranging from approximately 0.16 to 0.34 μm, with the highest concentration of 22 particles observed at a size of 0.23 μm. Similarly, in Figure 4c (PU/5%PANI), the particle size distribution spans from approximately 2.0 to 8.0 μm, with a peak concentration of 20 particles observed at a size of 3.5 μm. This thorough analysis provides valuable insights into the heterogeneous nature of particle sizes within the sample, thereby facilitating a comprehensive characterization of its particle size profile.

The surface topography of PU/PANI was examined using AFM, and representative topography images are depicted in Figure 5. In these images, the lighter shade corresponds to dispersed PANI particles, while the darker shade represents the continuous PU matrix. The 3D images captured for the pristine PU (Figure 5a) indicate a homogeneous polymeric film with a surface roughness of only 26.3 nm. Figure 5b illustrates the even dispersion of PANI at 1 wt.% in the PU matrix. This surface image suggests that the PANI was uniformly dispersed in the PU matrix without significant clusters, thus resulting in a surface roughness of 141 nm. Concerning composites with a higher PANI content, specifically at 3 wt.%, the composite surface exhibits a relatively uniform dispersion, as depicted in Figure 5c. While some PANI clumping is evident in 5 wt.% PANI, resulting in a surface roughness of approximately 415 nm, no conductive paths of the PANI manifested within the polymeric matrix. The findings indicate an increase in the surface roughness with a higher PANI content (Figure 5d). To mitigate agglomeration effects, it is noted that the practical maximum PANI content is approximately 3 wt.% in the PU matrix. Moreover, the favorable phase distribution observed with 3 wt.% PANI contributes to the interfacial charge density at the interface between the PANI particles and the PU host, potentially leading to an increase in the dielectric permittivity of the composites [26]. The findings from the AFM investigation align well with the results obtained through SEM visualization.

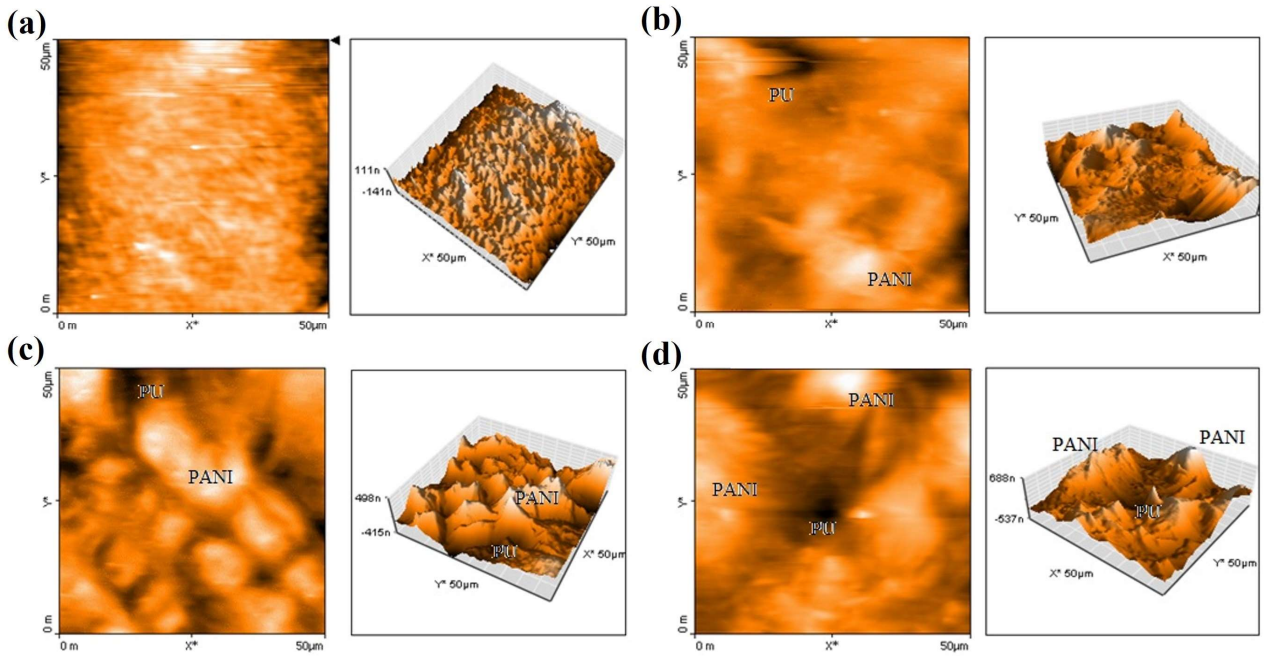

Figure 5. AFM topographies of the PU blended with PANI (a) neat PU, (b) PU/1%PANI, (c) PU/3%PANI, and (d) PU/5%PANI, respectively.

3.3. Effect of the PANI on the PU electrical properties

The relationship between frequency and dielectric permittivity is depicted in Figure 6. The permittivity is notably the highest at the lowest frequency and gradually diminishes with an increasing frequency. Generally, orientational polarization stands out as the dominant mechanism in the electric polarization of polar groups. It is well-established that the dielectric permittivity correlates with free dipoles oscillating in an alternating field. However, at low frequencies, both the orientational polarization and the space charge polarization come into play. Consequently, the permittivity consistently rises with the distribution of space charge in the PU/PANI composites. It is plausible that the PANI particles embedded in the polymer matrix serve as sources of space charge in the PU matrix. As the frequency increases, the dipoles start to lag behind the field, thus leading to a decrease in permittivity [27]. At sufficiently high frequencies, the dipoles can no longer keep pace with the rapid changes in the field direction. The observation of the loss tangent in composites with varying PANI content versus the frequency reveals that the loss tangent increases with an elevated concentration of the conductive filler in the matrix (Figure 7). Figure 8 illustrates the augmentation of ε_r with the PANI content at an operating frequency of 1 Hz.

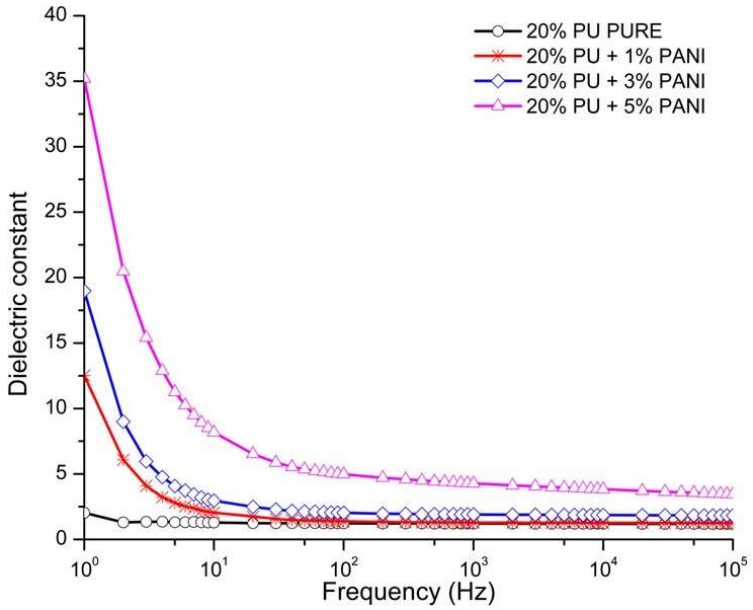

Figure 6. Plot shows the dielectric constant at various frequencies in relation to the PANI filler concentration.

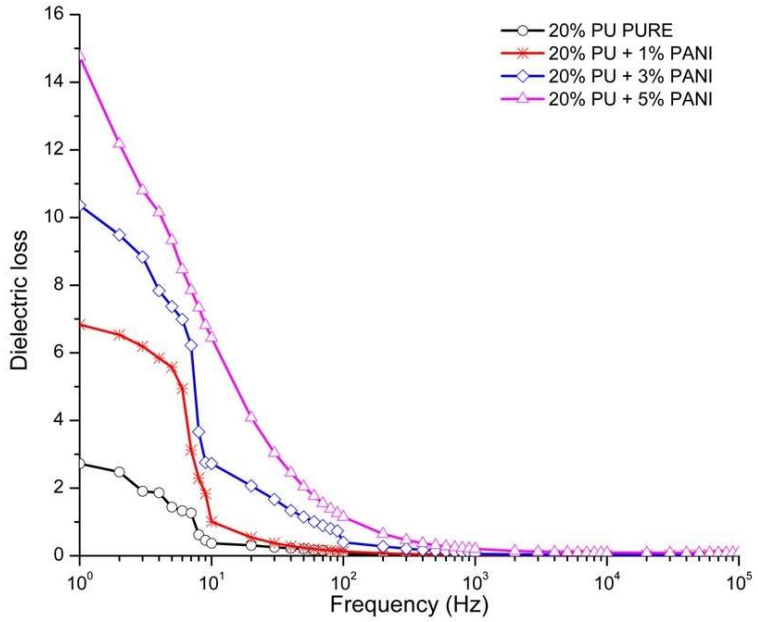

Figure 7. Dielectric loss at various frequencies in relation to the PANI filler concentration.

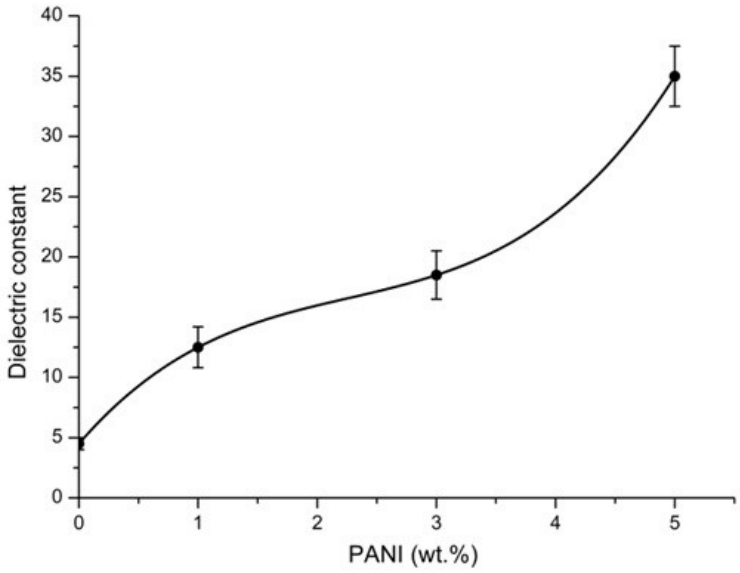

Figure 8. Plot shows the dielectric constant at 1 Hz driven frequency in relation to the PANI filler concentration.

For the neat PU, the dielectric constant exhibited its lowest value across all frequencies. The introduction of a conductive filler likely augmented the charge density. Both the permittivity and the conductivity exhibited enhancements attributed to the interface charges, thereby playing a dual role in contributing to conduction and inducing Maxwell-Wagner interfacial polarization [28]. Moreover, this polarization significantly influences the dielectric constant of the composite, which exhibited an increase corresponding to the quantity of the conductive filler. A comparative analysis of our findings and relevant literature results is presented in Table 1.

Table 1. Electrical and mechanical properties of PU/PANI composites from the literatures.

Authors and ref.	Fillers	ε_r (1 Hz)	σ (S/m, 100 Hz)	ξ (MPa)	M_{33} (m^2/V^2)
Putson C. et al. [12]	0% Cu	5.5 (at 100 Hz)	-	20.48	-
	2% Cu (nano)	7.5 (at 100 Hz)	-	22.42	-
	4% Cu (nano)	8.2 (at 100 Hz)	-	25.01	-
	6% Cu (nano)	10.0 (at 100 Hz)	-	29.82	-
	10% Cu (nano)	15.0 (at 100 Hz)	-	39.54	
Putson C. et al. [15]	PANI 0 wt.%	5.5 (at 100 Hz)	1.0×10^{-9}	-	-
	PANI 1 wt.%	10.2 (at 100 Hz)	0.5×10^{-8}	-	-
	PANI 3 wt.%	18.0 (at 100 Hz)	9.0×10^{-7}	-	-
	PANI 5 wt.%	43.5 (at100 Hz)	3.0×10^{-6}	-	-
Jaaoh D. et al. [29]	PANI 0 wt.%	8.0	0.34×10^{-11}	22.0	3.8×10^{-18}
	PANI 0.5 wt.%	14.8	0.89×10^{-11}	24.0	4.2×10^{-18}
	PANI 1.0 wt.%	19.5	1.52×10^{-11}	24.0	5.2×10^{-18}
	PANI 1.5 wt.%	21.5	4.67×10^{-11}	23.8	5.7×10^{-18}
	PANI 2.0 wt.%	23.5	3.79×10^{-11}	24.5	5.9×10^{-18}
Rabia S. et al. [18]	PANI 0 wt.%	-	0.1×10^{-6} (S/cm)	299.29	-
	PANI 0.1 wt.%	-	1.2×10^{-6} (S/cm)	346.97	-
	PANI 0.3 wt.%	-	1.5×10^{-6} (S/cm)	379.31	-
	PANI 0.5 wt.%	-	2.1×10^{-6} (S/cm)	376.98	-
	PANI 1.0 wt.%	-	7.0×10^{-6} (S/cm)	427.87	-
Our finding	PANI 0 wt.%	4.5	0.34×10^{-11}	20.14	1.19×10^{-18}
	PANI 1 wt.%	12.5	0.89×10^{-11}	20.32	4.61×10^{-18}
	PANI 3 wt.%	18.5	1.52×10^{-11}	20.76	7.06×10^{-18}
	PANI 5 wt.%	35.0	4.67×10^{-11}	21.18	13.80×10^{-18}

Figure 9 illustrates the frequency-dependent conductivity of the PU/PANI composite at room temperature. The conductivity curve exhibits a dispersion region in the high-frequency range, explained by a power law and a plateau (static value) in the low-frequency range, thus equalizing the direct current (DC) conductivity. Notably, the mechanical contribution to the conductivity in the DC regime is primarily attributed to the hopping transport of carriers between localized states, whereas the alternative current (AC) conductivity is associated with mobile charges between localized states and the orientation of the dipole moment. In our study, the composites' conductivity displays a substantial frequency independence with an increased filler content, as the dipolar contribution diminishes due to the suppressed molecular motions. However, the incorporation of conductive charge likely elevates the space charge density, in addition to that intrinsically induced by the presence of soft and hard segments within the PU matrix. Furthermore, the inevitable increase in the loss tangent is a consequence of the significantly heightened conductivity.

The PU/PANI composites exhibited electrical properties in the range of 0.1 to 3.0×10^{-8} S/m, as depicted in Figure 10. The PU/PANI composites are produced by amalgamating carbon-based materials such as PU with conducting polymers, namely PANI, to augment their conductivity and related properties. The introduction of PANI into carbon-based materials establishes a network of conductive pathways, thus facilitating an efficient electron movement and enhancing the overall conductivity of the PU/PANI composites [4]. These conductive pathways can be formed through diverse mechanisms, including the development of percolation networks or the integration of conductive fillers. The existence of such pathways empowers the PU/PANI composites to demonstrate electrical conductivity, akin to metals [12], while still preserving the inherent benefits of polymers, such as flexibility and lightweight properties.

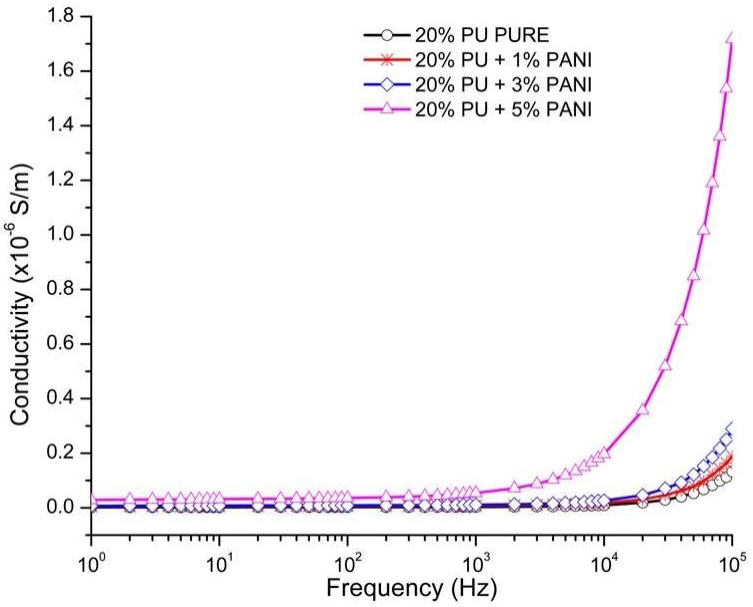

Figure 9. The conductivity of the composites with different PANI contents as a function of frequency.

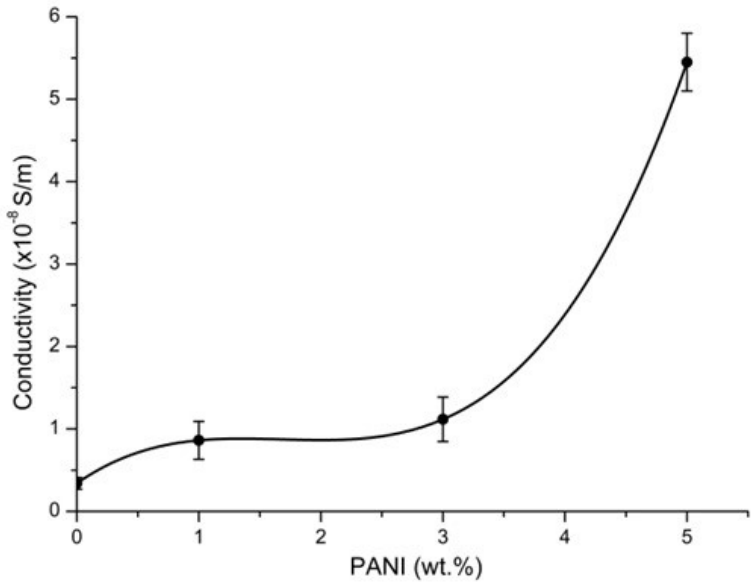

Figure 10. Conductivity at 1 kHz for blended PU/PANI composites with different weight fractions of PANI filler.

3.4. Effect of the PANI on the PU mechanical properties

The mechanical moduli of the blends are depicted in Figure 11. A marginal increase in the modulus is observed with the inclusion of the PANI content, attributed to the relatively low PANI quantities. The introduction of a small amount of conductive polymer into the PU matrix does not exert a significant impact on the elastic modulus in the PU/PANI blend, as illustrated in Figure 11. Existing

literature, as exemplified by Putson et al. [12], suggests a gradual decrease in the tensile strength with an elevated concentration of filler (Cu). However, our study indicates that PU/PANI blends may be more suitable to enhance the mechanical properties compared to PU/CU nano-particles.

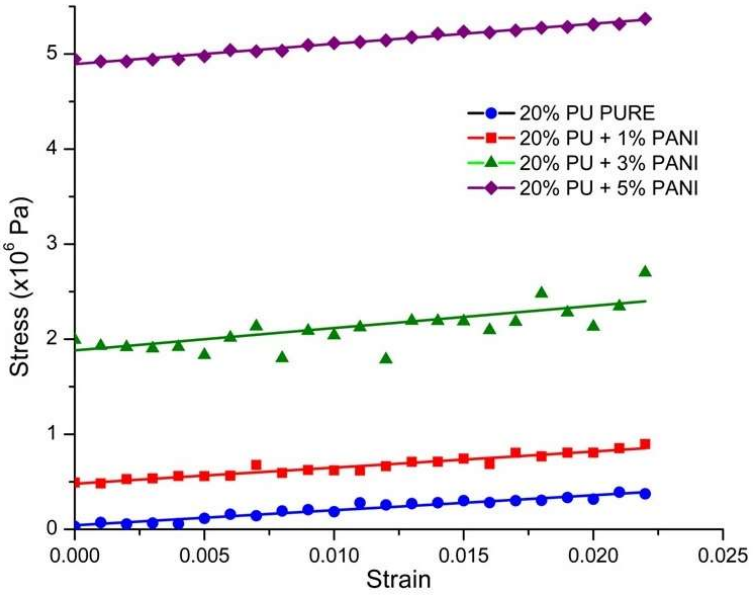

Figure 11. Plot of stress against strain for blended PU/PANI composites with varied PANI filler weight fractions.

The elastic moduli of both the neat PU and all composite materials are illustrated in Figure 12. As anticipated, an increment in the elastic modulus is observed with increasing PANI loading in all composites, reflecting the combined properties of the constituents. Notably, PU/5%PANI exhibits the highest modulus among the composites. The results further demonstrate that the PU/5%PANI composite presents a distinct advantage in the actuated strain under low electric fields. Additionally, saturation of the longitudinal strain is observed for PU/1%PANI, PU/3%PANI, and PU/5%PANI composites. The enhancement of mechanical properties in filled polymers is influenced by factors such as the filler type, volume fraction, dispersion, and interfacial adhesion between the filler and the matrix. Prior research indicates that the PU modulus filled with nano-sized Cu particles increased more than with micro-sized Cu particles, thus attributed to an improved interfacial adhesion [12]. The observed saturation of the longitudinal strain is not indicative of mechanical saturation within the sample, but rather points to the saturation of electrically induced polarization [23,30].

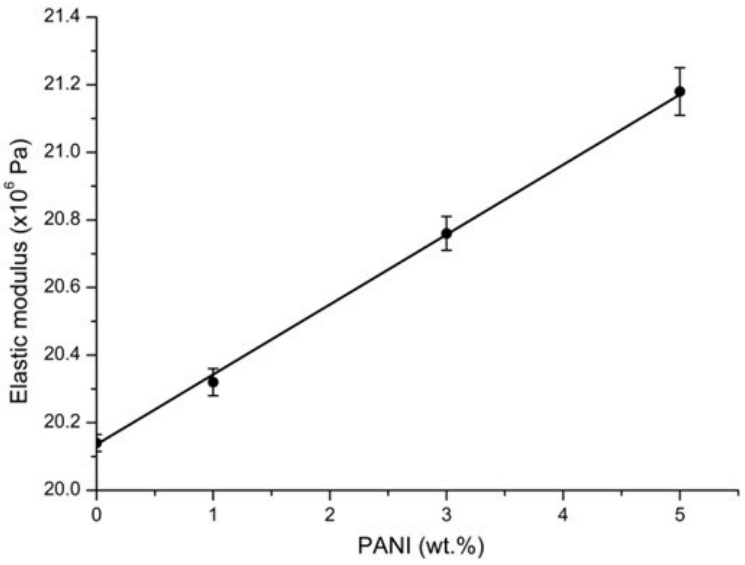

Figure 12. Elastic moduli of PU/PANI composites at different PANI weight fractions.

Additionally, Table 1 presents the anticipated mechanical and electrostrictive properties of the PU/PANI composites. The incorporation of 5 wt.% PANI results in an outstanding elastic modulus, making it promising for applications in living tissues. Moreover, the electrostrictive properties, represented by M_{33} and dielectric constant in the PU/5%PANI composite (Figure 6), demonstrate a high potential for converting mechanical signals into electrical signals. Guyomar et al. proposed a model to elucidate the influence of the dielectric constant and the saturation electrical field on M_{33} saturation in polyurethane-based composites. Their study investigated M_{33} variation concerning the thickness, composition, frequency, and electrical field, thus aligning with experimental data [31]. In our study, M_{33} calculations (Table 1) corroborate these findings. The combined mechanical and electrical properties of the PU/PANI composites are crucial in various medical applications, thus offering a unique advantage in medical devices where structural integrity and electrical conductivity are essential. Implants and wearable medical devices benefit from the composite's mechanical properties, ensuring durability and flexibility, while its electrical properties enable the integration of sensors, actuators, and electronic components [32]. In neurostimulation devices, the composite's mechanical strength ensures stability, while its electrical conductivity facilitates an effective signal transmission. The synergy between mechanical and electrical characteristics enhances the versatility of the PU/PANI composites in diverse medical applications, thus contributing to improved patient outcomes and healthcare technologies, including diagnostic tools that rely on both aspects, such as impedance-based diagnostics [7]. The conductivity of PU/PANI composites can be further elevated by optimizing the composition, morphology, and processing conditions of the composites, as illustrated in Figures 3–10. This characteristic holds promise for applications in tissue engineering, particularly in the field of medical device development [7].

Customizable composition and processing methods address specific medical requirements, thus ensuring an optimal performance and biocompatibility. However, additional research is needed, particularly in long-term biocompatibility and the optimization of electrical conductivity for enhanced stability. Standardization and regulatory considerations are crucial, involving the establishment of testing protocols and guidelines tailored to these composites, thus guaranteeing their safety and

efficacy in medical applications [33]. Exploration into the PU/PANI composite scaffolds for tissue engineering revealed their suitability for various applications, including neural and cardiac tissue engineering, where electrical stimulation proved beneficial. Despite their promising properties, the commercial utilization of PU/PANI scaffolds in tissue engineering remains limited due to challenges such as scalability, long-term material stability, and the need to address diverse tissue requirements [7]. Ongoing research endeavors aim to overcome these limitations, thus unlocking the full potential of PU/PANI in practical biomedical applications and contributing to the progress of biomedical technology.

4. Conclusions

In this study, we synthesized composite films comprised of an elastic polymer matrix of PU with dispersed conductive PANI polymer. Our investigation focused on examining the mechanical and electrical properties, specifically the electrical conversion capability, of these PU/PANI composites across varying PANI content ranges. A microscopic analysis revealed homogenous distribution of PANI in the PU matrix up to approximately 3 wt.%, beyond which, at 5 wt.%, inhomogeneity was observed, setting the upper limit for our experiments. The dielectric constant, loss tangent, and conductivity exhibited a decreasing trend with an increase in the driving frequency. Conversely, for comparative purposes, the dielectric and conductivity values increased with higher PANI contents. Notably, the elastic modulus of the composites demonstrated an increasing trend with the filler content. The experimental findings highlight the superior performance of the PU/PANI composites over the neat PU in terms of mechanical-to-electrical conversion, thus suggesting promising applications in the field of medical tissue engineering utilizing conductive PU/PANI polymers.

Use of AI tools declaration

The authors declare they have not used Artificial Intelligence (AI) tools in the creation of this article.

Acknowledgments

The authors are grateful to the Faculty of Science at Sriracha, Kasetsart University, Sriracha Campus thought the funding No. Sci-Src-G01/2565 and Sci-Src-G01/2567.

Conflict of interest

The authors declare no conflict of interest.

References

1. Grand View Research (2020) Polyurethane foam market size, share & trends analysis report by product (rigid foam, flexible foam), by application (bedding & furniture, transportation, packaging, construction, electronics, footwear), by region, and segment forecasts. Available from: https://www.grandviewresearch.com/industry-analysis/polyurethane-foam-market.

2. Bar-Cohen Y, Leary S, Harrison J, et al. (1999) Electroactive polymer (EAP) actuation of mechanisms and robotic devices. The 10th International Conference on Solid-state Sensors and Actuators, Sendai, Japan, June 7–10.
3. Akindoyo JO, Beg M, Ghazali S, et al. (2016) Polyurethane types, synthesis and applications—A review. *Rsc Adv* 6: 114453–114482. https://doi.org/10.1039/C6RA14525F
4. Naveen MH, Gurudatt NG, Shim YB (2017) Applications of conducting polymer composites to electrochemical sensors: A review. *Appl Mater Today* 9: 419–433. http://dx.doi.org/10.1016/j.apmt.2017.09.001
5. Sobczak M, Kędra K (2022) Biomedical polyurethanes for anti-cancer drug delivery systems: A brief, comprehensive review. *Int J Mol Sci* 23: 8181. https://doi.org/10.3390/ijms23158181
6. Jaaoh D, Putson C, Muensit N (2015) Deformation on segment-structure of electrostrictive polyurethane/polyaniline blends. *Polym J* 61: 123–130. http://dx.doi.org/10.1016/j.polymer.2015.01.081
7. Zare EN, Makvandi P, Ashtari B, et al. (2019) Progress in conductive polyaniline-based nanocomposites for biomedical applications: A review. *J Med Chem* 63: 1–22. https://doi.org/10.1021/acs.jmedchem.9b00803
8. Rai R, Roether JA, Boccaccini AR (2022) Polyaniline based polymers in tissue engineering applications: a review. *Prog Biomed Eng* 4: 042004. https://doi.org/10.1088/2516-1091/ac93d3
9. Cruz-Pacheco AF, Paredes-Madrid L, Orozco J, et al. (2020) Assessing the influence of the sourcing voltage on polyaniline composites for stress sensing applications. *Polymers* 12: 1164. doi:10.3390/polym12051164
10. Kumar SKS, Prakash C (2021) Characterization of electrospun polyurethane/polyacrylonitrile nanofiber for protective textiles. *Iran Polym J* 30: 1263–1271. https://doi.org/10.1007/s13726-021-00961-6
11. Kazemi F, Naghib S, Mohammadpour Z (2020) Multifunctional micro-/nanoscaled structures based on polyaniline: An overview of modern emerging devices. *Mater Today Chem* 16: 100249. https://doi.org/10.1016/j.mtchem.2020.100249
12. Putson C, Jaaoh D, Meauma N, et al. (2012) Effect of micro-and nano-particle fillers at low percolation threshold on the dielectric and mechanical properties of polyurethane/copper composites. *J Inorg Organomet Polym* 22: 1300–1307. https://doi.org/10.1007/s10904-012-9755-z
13. Pierini F, Lanzi M, Lesci IG, et al. (2015) Comparison between inorganic geomimetic chrysotile and multiwalled carbon nanotubes in the preparation of one-dimensional conducting polymer nanocomposites. *Fibers Polym* 16: 426–433. https://doi.org/10.1007/s12221-015-0426-x
14. Pierini F, Lanzi M, Nakielski P, et al. (2017) Electrospun polyaniline-based composite nanofibers: Tuning the electrical conductivity by tailoring the structure of thiol-protected metal nanoparticles. *J Nanomater* 2017: 6142140. https://doi.org/10.1155/2017/6142140
15. Putson C, Jaaoh D, Muensit N (2013) Interface polarization effect on dielectric and electrical properties of polyurethane (PU)/polyaniline (PANI) polymer composites. *Adv Mat Res* 770: 275–278. https://doi.org/10.4028/www.scientific.net/AMR.770.275
16. Milakin KA, Morávková Z, Acharya U, et al. (2021) Enhancement of conductivity, mechanical and biological properties of polyaniline-poly (N-vinylpyrrolidone) cryogels by phytic acid. *Polym J* 217: 123450. https://doi.org/10.1016/j.polymer.2021.123450

17. Rahman MM, Mahtab T, Mukhlish MZB, et al. (2021) Enhancement of electrical properties of metal doped polyaniline synthesized by different doping techniques. *Polym Bull* 78: 5379–5397. https://doi.org/10.1007/s00289-020-03389-9
18. Sattar R, Kausar A, Siddiq M (2015) Thermal, mechanical and electrical studies of novel shape memory polyurethane/polyaniline blends. *Chin J Polym Sci* 33: 1313–1324. https://doi.org/10.1007/s10118-015-1680-5
19. Dubey AK GS, Basu B (2011) Optimization of electrical stimulation parameters for enhanced cell proliferation on biomaterial surfaces. *J Biomed Mater Res B Appl Biomater* 98: 18–29. https://doi.org/10.1002/jbm.b.31827
20. Stejskal J, Gilbert R (2002) Polyaniline. Preparation of a conducting polymer (IUPAC technical report). *Pure Appl Chem* 74: 857–867. https://doi.org/10.1351/pac200274050857
21. Griffiths DJ (2014) *Introduction to Electrodynamics: Pearson New International Edition*, New York: Pearson.
22. Agilent Technologies (2006) Agilent basics of measuring the dielectric properties of materials. Available from: https://academy.cba.mit.edu/classes/input_devices/meas.pdf.
23. Nawaka K, Putson C (2020) Enhanced electric field induced strain in electrostrictive polyurethane composites fibers with polyaniline (emeraldine salt) spider-web network. *Compos Sci Technol* 198: 108293. https://doi.org/10.1016/j.compscitech.2020.108293
24. Rangel-Vázquez NA, Salgado-Delgado R, García-Hernández E, et al. (2009) Characterization of copolymer based in polyurethane and polyaniline (PU/PANI). *J Mex Chem Soc* 53: 248–252. https://doi.org/10.29356/jmcs.v53i4.979
25. Jiang L, Betts A, Kennedy D, et al. (2015) Improving the electromechanical performance of dielectric elastomers using silicone rubber and dopamine coated barium titanate. *Mater Des* 85: 733–742. http://dx.doi.org/10.1016/j.matdes.2015.07.075
26. Liang X, Deng Y, Li S, et al. (2022) Waterborne polyurethane-acrylate-polyaniline: Interfacial hydrogen bonding for enhancing the antistatic, damping, and mechanical properties. *Polym Adv Technol* 33: 2667–2681. https://doi.org/10.1002/pat.5722
27. Rai R, Sharma S, Rani R, et al. (2014) Dielectric and magnetic studies of $(NKNLS)_{1-x}$–$(NZFO)_x$ multiferroic composites. *J Alloys Compd* 614: 277–282. http://dx.doi.org/10.1016/j.jallcom.2014.06.051
28. Bobnar V, Levstik A, Huang C, et al. (2007) Enhanced dielectric response in all-organic polyaniline–poly (vinylidene fluoride-trifluoroethylene-chlorotrifluoroethylene) composite. *J Non-Cryst Solids* 353: 205–209. https://doi.org/10.1016/j.jnoncrysol.2006.10.003
29. Jaaoh D, Putson C, Muensit N (2014) Contribution of electrostriction in polyurethane/polyaniline blends. *Adv Mat Res* 1025–1026: 697–702. https://doi.org/10.4028/www.scientific.net/AMR.1025-1026.697
30. Guyomar D, Yuse K, Cottinet PJ, et al. (2010) Focus on the electrical field-induced strain of electroactive polymers and the observed saturation. *J Appl Phys* 108: 114910. https://doi.org/10.1063/1.3504601
31. Guyomar D, Cottinet PJ, Lebrun L, et al. (2012) The compressive electrical field electrostrictive coefficient M33 of electroactive polymer composites and its saturation versus electrical field, polymer thickness, frequency, and fillers. *Polym Adv Technol* 23: 946–950. https://doi.org/10.1002/pat.1993

32. Pina CD, Falletta E (2022) Advances in polyaniline for biomedical applications. *Curr Med Chem* 29: 329–357. https://doi.org/10.2174/0929867328666210419135519
33. Jirakittidul K, Limthin D, Mahithithummathorn S, et al. (2023) Effects of annealing temperature and time on properties of thermoplastic polyurethane based on different soft segments/multi-walled carbon nanotube nanocomposites. *Polymers* 15: 364. https://doi.org/10.3390/polym15020364

AIMS Press